Synthesis and Physicochemical Characterization of an Aluminosilicate Zeolite with IFR Topology, Prepared by the Fluoride Route

L. A. Villaescusa,[†,§] P. A. Barrett,[†,||] Martin Kalwei,[‡] Hubert Koller,[‡] and M. A. Camblor*[,†,⊥]

Instituto de Tecnología Química, CSIC−UPV, Universidad Politécnica de Valencia, Avda. Los Naranjos s/n, 46022 Valencia, Spain, and Institut für Physikalische Chemie, Westfälische Wilhelms-Universität Münster, Schlossplatz 4/7, D-48149 Münster, Germany

Received September 22, 2000. Revised Manuscript Received December 11, 2000

An aluminosilicate zeolite with IFR topology can be synthesized in a wide range of Si/Al ratios (Si/Al ≥ 20) using benzylquinuclidinium as a structure-directing agent in the presence of fluoride anions. The phase selectivity of the crystallization depends on both the Al and the water content of the synthesis mixture, and by adjustment of the degree of dilution of the mixture, it is also possible to obtain zeolite Beta. The isomorphous substitution of Si by Al in the IFR framework and the acidity of the calcined zeolite has been confirmed by a number of physicochemical techniques. The calcined IFR material contains acid sites of medium strength with large pores and a large void volume. Partial dealumination occurs during calcination, but N_2 and pyridine adsorption experiments do not indicate any pore blocking. The aluminosilicate IFR zeolite contains unusual acid sites that are involved in relatively strong hydrogen bonds. Besides the well-known ^{1}H NMR chemical shift for acid sites at 3.9 ppm and the IR band at 3629 cm^{-1}, the hydrogen-bonded acid sites are characterized by ^{1}H NMR chemical shifts of 5.2 and 6.3 ppm and a broad unresolved IR band at 3488 cm^{-1}.

Introduction

The synthesis of novel zeolitic materials is an important field of active scientific research because of the potential applications of new structures or compositions in catalysis and adsorption processes. Side by side along with the search for new structures comes the need to investigate more fundamental issues such as understanding the key factors that govern the phase selectivity during the crystallization of zeolites. New pore systems featuring special characteristics for example in terms of channel size and dimensionality, or by virtue of the presence of cages, etc., can show specific shape selectivity properties in both catalysis and adsorption processes. Additionally, nonstructural properties, such as the chemical composition, can also modify the reactive and adsorptive properties of the materials considerably. Therefore, the development of new processes or the improvement of existing ones will certainly benefit from the development and characterization of novel zeolitic materials, especially because at present the a priori design of microporous materials for specific applications still lies beyond the current potential of zeolite scientists.

We recently reported the synthesis and structure[1] of a pure silica zeolite, named ITQ-4. Its new topology has been assigned the structure code IFR by the International Zeolite Association.[2] ITQ-4 is characterized by a very high void volume and by its unique one-dimensional sinusoidal 12-membered ring (MR) channel, and it is isotypical with the borosilicate and aluminosilicate materials SSZ-42[3] and MCM-58.[4] In this work we report on the introduction of Al into the IFR framework by the fluoride synthesis route. The resulting material[5] will be denoted as Al-ITQ-4 throughout this paper to distinguish it from the materials prepared by the hydroxide synthesis route. Al-ITQ-4 is an attractive material for applications in a range of catalytic processes due to the unique IFR topology and the compositional flexibility provided by the fluoride synthesis method. SSZ-42 is described in the open literature as a borosilicate that is synthesized in the presence of sodium cations, and it can be converted to an aluminosilicate by postsynthesis treatment of the calcined material with an aqueous

* To whom correspondence should be addressed.
† Universidad Politécnica de Valencia.
‡ Westfälische Wilhelms-Universität Münster.
§ Current address: School of Chemistry, University of St. Andrews, St. Andrews, Scotland, KY16 9ST.
|| Current address: Praxair Inc., 175 East Park Drive, P.O. Box 44, Tonawanda, NY 14150-7891.
⊥ Current address: Industrias Químicas del Ebro, Polígono de Malpica, D Street, 97, 50057, Zaragoza, Spain. E-mail: macamblor@iqe.es. Phone: 34-976-573625. Fax: 34-976-572557.

(1) (a) Camblor, M. A.; Corma, A.; Villaescusa, L. A. *Chem. Commun.* **1997**, 749. (b) Barrett, P. A.; Camblor, M. A.; Corma, A.; Jones, R. H.; Villaescusa, L. A. *Chem. Mater.* **1997**, *9*, 1713.
(2) http://www.iza-structure.org/databases/.
(3) Zones, S. I.; Rainis, A. PCT/US95/01412, 1995.
(4) Valyocsik, E. W. U.S. Patent 5437855, 1995.
(5) Villaescusa, L. A.; Camblor, M. A.; Corma, A. Spanish Patent 9602685, 1996.

10.1021/cm001180e CCC: $20.00
Published on Web 06/07/2001

aluminum nitrate solution.[6] As-made MCM-58 is an aluminosilicate that can be crystallized as a pure phase with an Si/Al ratio of 19[7] (Si/Al between 12 and 33 according to the patent).[4] What makes ITQ-4 different from SSZ-42 and MCM-58 is the use of fluoride ions as the mineralizing agent in the synthesis of ITQ-4 and, as will be shown here, the larger range in Si/Al ratios attainable by direct synthesis compared to that of MCM-58. These synthetic factors can influence the physicochemical and catalytic properties, and it is the objective of this report to present a comprehensive physicochemical characterization of Al-ITQ-4.

Experimental Section

Materials. The synthesis of the ITQ-4 samples was carried out hydrothermally using the previously reported procedure for pure silica ITQ-4,[8] with F^- as a mineralizer and *N*-benzylquinuclidinium (BQ) as a structure-directing agent (SDA). The only modification with respect to the procedure for pure silica ITQ-4 is that here varying amounts of aluminum were introduced into the crystallizing mixture. Al isopropoxide was dissolved in a solution of the hydroxide form of the SDA prior to the hydrolysis of the tetraethyl orthosilicate used as a source of SiO_2. Unless otherwise stated, the overall composition of the starting mixtures was

$$SiO_2{:}xAl_2O_3{:}(0.5{+}2x)BQ(OH){:}0.5HF{:}wH_2O$$

with $x = 0-0.11$ and $w = 3.6-15$, BQ(OH) being *N*-benzylquinuclidinium hydroxide. The crystallizations were carried out in Teflon-lined stainless steel autoclaves under rotation (60 rpm) at 423 or 448 K. In some cases, an ultrasonicated suspension of ITQ-4 crystals in water was added to serve as seeds for the crystallization, and the mixture was further stirred at the end of the preparation process.

Characterization. Phase purity and crystallinity were determined by conventional powder X-ray diffraction (XRD) using a Philips X'Pert diffractometer (Cu Kα radiation provided by a graphite monochromator). The unit cell size was determined by model-independent full-profile fitting[9] of the diffractograms. C, H, and N contents were determined with a Carlo Erba 1106 elemental analyzer. The Al content was determined by atomic absorption. The fluoride content was determined using an ion-selective electrode connected to a Mettler Toledo 355 ion analyzer after dissolution of the as-made solids by a standard procedure.[10] ^{29}Si and ^{27}Al MAS NMR spectra of the solids were recorded on a Varian VXR 400SWB spectrometer. The ^{29}Si MAS NMR spectra were recorded with a spinning rate of 5.5 kHz at a ^{29}Si frequency of 79.459 MHz with a 55.4° pulse length of 4.0 μs and a recycle delay of 60 s. ^{27}Al MAS NMR were recorded at a frequency of 104.218 MHz with a spinning rate of 7 kHz with a 9° pulse length (liquid reference sample) of 0.5 μs and a recycle delay of 0.5 s. ^1H MAS and static ^{27}Al NMR spectra were recorded on a Bruker DSX-500 spectrometer. ^1H-^{27}Al REAPDOR experiments were performed on the same spectrometer with 8-kHz sample spinning using ^1H π pulse lengths of 9.6 μs for the spin−echo. ^{27}Al irradiation was carried out with $\nu_{rf} = 59$ kHz and a REAPDOR dephasing pulse length of 100 μs. ^{29}Si and ^1H chemical shifts are reported relative to TMS and ^{27}Al was calibrated with $Al(H_2O)_6^{3+}$. For the NMR studies on the acid sites the calcined samples were dehydrated according to the following procedure: First, the powders were evacuated overnight at room temperature. Then, they were heated by an overall rate of 2 K/min to a final temperature of 723 K, and activated for 12 h. During the heating process, two stops were made for 2 h at 353 and 433 K. The samples were sealed under vacuum and reopened in a drybox under argon gas to fill the airtight NMR rotors. N_2 adsorption/desorption experiments were undertaken isothermally at 77 K using an automatic ASAP 2000 Micromeritics apparatus. The infrared spectra were recorded using a Nicolet 710 FTIR spectrometer using self-supported wafers. Spectra were obtained at room temperature after outgassing the materials overnight at 673 K under dynamic vacuum of 10^{-3} Pa and after adsorption of pyridine at room temperature and outgassing under vacuum at 523, 623, and 673 K, respectively. The acidity was also characterized by temperature-programmed desorption of ammonia (TPD) using a Micromeritics TPR/TPD 2900. Around 200 mg of zeolite was heated at 723 K at a heating rate of 10 K/min in an oxygen flow and then kept at this temperature for 1 h. Then, the sample was cooled to 373 K in a He flow (100 mL/min). After this temperature was reached, pulses of NH_3 in He were introduced up to saturation of the sample. Then, the sample was heated from 373 to 1173 K while the desorption was monitored by conductivity. The total volume of NH_3 adsorbed on the zeolite in standard conditions was assumed to be equal to the total amount of NH_3 desorbed. Finally, crystal size and morphology were monitored by scanning electron microscopy (SEM) using a JEOL JSM-6300 microscope.

Table 1. Summary of Synthesis Conditions and Results for $H_2O/SiO_2 = 15$[a]

run	Al/(Si + Al) × 100 in gel	temp/K	time/days	solid
L228	0	408	19	ITQ-4 > 5%
L248B	6.25	408	13	amorphous
			49	Lb + ITQ-4
L269	0	423	13	ITQ-4
L428[b]	1.05	423	9	ITQ-4
L406[b]	2.05	423	8	ITQ-4
L245[b]	2.56	423	7	ITQ-4
L244	2.63	423	15	ITQ-4 +(Lb)
			31	ITQ-4
L233	3.22	423	11	Lb
L243			20	ITQ-4 + (Lb)
MD248[b]	3.70	423	18	ITQ-4
L249	6.25	423	22	amorphous
			49	ITQ-4 + Lb
L315[c]	4.43	448	13	ITQ-4
L250	6.29	448	9	amorphous
			22	ITQ-4
L316[c]	7.93	448	23	ITQ-4
L346[c]	7.95	448	31	ITQ-4+Lb
			36	ITQ-4
L294	8.1	448	24	Lb + ITQ-4
			39	ITQ-4 + Lb
L526	10	448	14	Beta
			36	Beta

[a] Lb is a material with an XRD pattern resembling those of MWW zeolites (Figure 1). [b] Seeds of pure silica ITQ-4 crystallites were used (3−5 mass % with respect to the total amount of silica). [c] Seeds of aluminosilicate (Si/Al = 20) ITQ-4 crystallites were used (3−5 mass % with respect to the total amount of silica).

Results and Discussion

Synthesis. In Table 1 a summary of synthesis conditions and results for $H_2O/SiO_2 = 15$ is given. Under these synthesis conditions we were able to obtain highly crystalline ITQ-4 materials with Si/Al ratios in the 20−∞ range. The range of Si/Al ratios obtained for ITQ-4

(6) Chen, C. Y.; Finger, L. W.; Medrud, R. C.; Kibby, C. L.; Crozier, P. A.; Chan, I. Y.; Harris, T. V.; Beck, L. W.; Zones, S. I. *Chem. Eur. J.* **1998**, *4*, 1310.
(7) Ernst, S.; Hunger, M.; Weitkamp, J. *Chem. Ing. Tech.* **1997**, *69*, 77.
(8) Barrett, P. A.; Camblor, M. A.; Corma, A.; Jones, R. H.; Villaescusa, L. A. *J. Phys. Chem. B* **1998**, *102*, 4147.
(9) Murray, A. D.; Fitch, A. N. Mprofil Program for Le Bail Decomposition and Profile Refinement, 1990.
(10) Guth, J. L.; Wey, R. *Bull. Soc. Fr. Minéral. Cristallogr.* **1969**, *92*, 105.

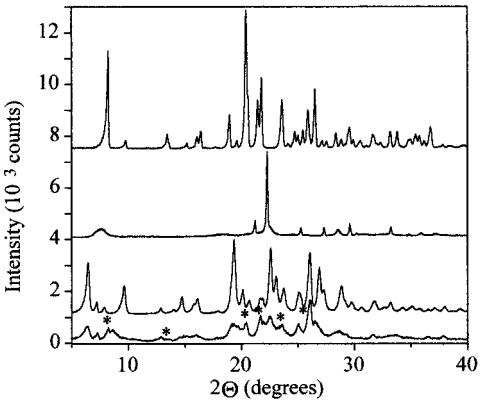

Figure 1. X-ray diffraction patterns of crystalline as-made phases relevant to this work: (from bottom to top) the phase named Lb in Table 1, ITQ-1[13] (shown for comparison), the pure silica Beta synthesized with benzylquinuclidinium and ITQ-4. Reflections marked with * are coincident with ITQ-4 reflections.

significantly extends the known range of attainable Si/Al ratios, based on direct synthesis, for the isomorphous SSZ-42[3] and MCM-58[4] materials, and must be ascribed to the different synthetic procedure employed for ITQ-4 (presence of F^- and absence of alkali cations). When the amount of Al in the crystallization mixture of ITQ-4 is further increased (Si/Al $\leq$10 for $H_2O/SiO_2 = 15$ and $T = 448$ K), zeolite Beta crystallized instead of ITQ-4. The crystallization of either ITQ-4 or zeolite Beta illustrates the apparent ability of the large *N*-benzylquinuclidinium cation to direct the synthesis to form large 12 MR pore materials. The effect of Al on the phase selectivity of the crystallization will be commented below in connection with the effect of the water content.

For $H_2O/SiO_2 = 15$ (Table 1) and Si/Al $\geq$ 11 we did not observe competition with other phases in the presence of seeds, while in their absence a phase (termed Lb in Table 1) with an XRD pattern resembling that of the as-made precursor of the MCM-22[11]/SSZ-25[12]/ITQ-1[13] family of zeolites (Figure 1) competed under certain conditions with zeolite ITQ-4. At long crystallization times, however, this phase dissolves as ITQ-4 crystallizes and it is unfavored also by increasing the crystallization temperature and decreasing the Al contents (Table 1). However, in contrast to the layered precursors of MCM-22, SSZ-25, and ITQ-1, the layered material converted to an almost amorphous phase upon calcination to 853 K.

As shown in Figure 2, the Al molar fraction in the zeolite product closely matches that of the synthesis mixture for molar fractions up to about 4%. For higher Al contents the effectiveness of the Al incorporation diminishes and the curve in Figure 2 flattens to a constant value of around 5% (around 1.6 Al per unit cell of 32 tetrahedral atoms). This is close to, but smaller than, the expected limit of Al incorporation into ITQ-4 under these synthesis conditions (*N*-benzylquinuclidinium as SDA in the absence of alkali cations), which

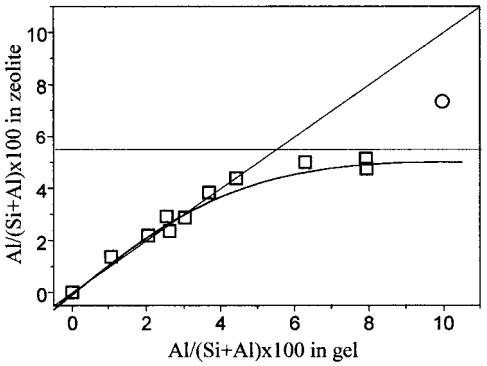

Figure 2. Molar fraction of Al in zeolite vs gel for ITQ-4 (squares) and Beta (circles).

Table 2. Synthesis Conditions and Results at 448 K with Varying Al and Water Contents

run	H_2O/SiO_2	Al/(Al + Si) × 100	time (days)	product
L250	15	6.2	9	amorphous
			22	ITQ-4
L526	15	10	14	Beta
			35	Beta
L496	7.5	0	6	ITQ-4
L400	7.5	2.6	6	Beta
L405	4.5	0	6	ITQ-4
L442	3.6	0	1	Beta
			6	Beta

is 2Al/uc from charge balance considerations (because in ITQ-4 only two *N*-benzylquinuclidinium cations can be accommodated per unit cell of 32 T atoms).[8] The fact that we do not reach that limit may just reflect a competition between $[AlO_{4/2}]^-$ and F^- for incorporation into the solid. The role and location of F in pure silica ITQ-4 have been previously discussed.[8] In contrast, when the phase that crystallizes is zeolite Beta, a larger fraction of Al is found in the zeolite (Figure 2).

Crystallization of ITQ-4 or Zeolite Beta as a Function of Al Content and Degree of Dilution of the Synthesis Mixture. At a first glance, the crystallization of zeolite Beta instead of ITQ-4 when the Si/Al ratio in the synthesis mixture is decreased to 10 (Table 1) could be simply rationalized in terms of those charge balance considerations: a zeolite with a three-dimensional 12MR large pore system may accommodate a greater concentration of organic cations (around 5 per unit cell of 64 T atoms, according to the chemical analyses for the pure silica Beta: 1.34% N, 16.30% C, 1.54% F) and hence a larger concentration of framework Al (Si/Al = 13, or 4.6Al/uc) than the monodimensional large pore ITQ-4. However, we will show next that the system is not that simple and that the same result (crystallization of Beta instead of ITQ-4) may be realized for Si/Al ratios well above the limit for ITQ-4 and even for pure silica compositions if the H_2O/SiO_2 ratio in the initial mixture is conveniently decreased.

As shown in Table 2, decreasing the water content in the initial mixture narrows the crystallization field of ITQ-4 and widens that of zeolite Beta with respect to the Al content. Thus, for Si/Al = 38 a decrease in the H_2O/SiO_2 ratio from 15 to 7.5 changes the product of the crystallization from ITQ-4 to zeolite Beta. For pure silica compositions it is necessary to further decrease the H_2O/SiO_2 ratio below 4 to obtain zeolite Beta. Obviously, these results can no longer be rationalized in terms of charge balance considerations of the whole

(11) Lawton, S. L.; Fung, A. S.; Kennedy, G. J.; Alemany, L. B.; Chang, C. D.; Hatzikos, G. H.; Lissy, D. N.; Rubin, M. K.; Timken, H. C.; Steuernagel, S.; Woessner, D. E. *J. Phys. Chem.* **1996**, *100*, 3788.
(12) Chan, I. Y.; Labun, P. A.; Pan, M.; Zones, S. I. *Microporous Mater.* **1995**, *3*, 409.
(13) Camblor, M. A.; Corma, A.; Díaz-Cabañas, M. J.; Baerlocher, Ch. *J. Phys. Chem.* **1998**, *102*, 44.

Table 3. Crystallinity, Aluminum Content, and Yield of Solids during Crystallization at 448 K of a Starting Mixture with Si/Al = 38 and H_2O/SiO_2 = 7.5

time (days)	yield (mass %)	Si/Al in solid	product
0.3	21.5	41	amorphous
0.9	22.5	39	amorphous
1.9	21.6	38	Beta (<25%)
3.2	18.9	38	Beta

reaction mixture. However, charge balance in the nuclei could still be determining the overall phase selectivity. We have checked that during the course of a crystallization with an overall Si/Al = 38 there is a change in the yield of solids but not a change in their Si/Al ratio, which were basically identical to that of the whole reaction mixture (Table 3) and thus well above the limit for ITQ-4. This observation rules out that the observed phase selectivity change were due to a low Si/Al ratio in the crystallizing liquor (or in the amorphous solid) during the nucleation step that could promote the nucleation of a phase (i.e., Beta) which is able to accommodate a larger Al content.

Generally, an increase in the Al content produces the same effect as a decrease in the water content.[14] In an attempt to understand better these phase selectivity changes, we have now considered what is the effect of varying the SDA and F concentrations in the synthesis of ITQ-4.

Under the synthesis conditions described, the organic cation is deemed to be the most soluble component, so a decrease in the water/silica ratio may have as its primary and main effect an increase in the concentration of benzylquinuclidinium in the liquid phase of the crystallizing mixture. The first three rows in Table 4 may be used to compare the effect of an increase in the overall concentration with that of an increase in the concentration of the organic cation. When the H_2O/SiO_2 is reduced by around a half from 7.5 to 3.6, the selectivity changes from ITQ-4 to Beta. Similarly, when the concentration of benzylquinuclidinium is doubled while keeping the H_2O/SiO_2 ratio constant, the main product is also Beta, although there is also a small and persistent amount of ITQ-4 found in the product and we also note an unexpected decrease in the yield of zeolite. This phase selectivity change suggests that the increase in concentration of the SDA may be the main, but not unique, reason for the change in selectivity observed when the H_2O/SiO_2 ratio is decreased. Our most frequent observation in the synthesis of silica phases using a large number of different SDAs is that a decrease in the H_2O/SiO_2 ratio changes the selectivity to a phase of lower framework density and larger organic content.[14] Thus, one can argue that an increase in the concentration of the organic cation favors the crystallization of a phase able to accommodate a larger concentration of those cations. There are, however, exceptions to this trend because we have found changes of selectivity between phases with the same organic content (like ITE and STF).[14]

On the other hand, the H_2O/SiO_2 ratio may also have an effect on the F^- concentration and the effect may be dramatic when the Al content is varied. Because F^- forms stable complexes with Al, an increase in the Al concentration may cause a large decrease in the effective concentration of F^- available for the crystallization. The effect of adding aluminum or varying the overall concentration of fluoride is shown in the last rows of Table 4. For a constant H_2O/SiO_2 ratio of 7.5, the addition of Al (Si/Al = 38) changes the phase selectivity of the crystallization from ITQ-4 to Beta. However, the product of the crystallization does not change when the fluoride content is increased or decreased. The only effects observed are a decrease in the yield of zeolite upon increasing the F^- content, presumably due to the increased formation of soluble fluorosilicate species, and the incomplete crystallization of the mixture when the F/Si ratio (0.075) approaches the level ideally found in the zeolite (0.0625).

Thus, depending on the degree of concentration of the reaction mixture, when benzylquinuclidinium is used, it is possible to crystallize zeolite Beta in a wide range of Si/Al ratios (from no Al to Si/Al around 10).

Characterization. The chemical composition of several ITQ-4 samples synthesized from reaction mixtures containing *N*-benzylquinuclidinium, fluoride anions, and varying amounts of Al are listed in Table 5. The C/N ratio is close to the value for the organic additive (14, with only a small but non-negligible deviation for the sample with the highest Al content), suggesting the structure-directing agent is occluded essentially intact inside the zeolitic pores. This was further confirmed by ^{13}C CPMAS NMR spectroscopy and by the structure solution of as-made pure silica ITQ-4, which showed the location of the benzylquinuclidinium cations inside the large pore channels with a close correspondence between the bent shape of the cation and the sinusoidal pore geometry.[8] Chemical analysis indicates that around two molecules per unit cell of 32 T atoms are occluded in all the samples after the synthesis. In the defect-free pure silica material the positive charge of the organic cation is balanced by the equivalent amount of F^- anions, and the ideal chemical composition is $[C_{14}NH_{20}F]_2[Si_{32}O_{64}]$.[8] The fluoride anions were very recently located inside the small $[4^35^26]$ cages within the zeolite walls,[8] and multinuclear NMR analysis revealed a strong interaction between F and different Si sites at room temperature.[15]

However, as Al is introduced into the material, the amount of fluorine decreases (Table 5), suggesting that the isomorphous substitution can be formally regarded as if $[AlO_{4/2}]^-$ tetrahedra (see NMR below) substitutes for $[SiO_{4/2}F]^-$ units in the framework. Thus, the ideal chemical composition for the aluminosilicate is $[C_{14}NH_{20}F_{(1-x/2)}]_2[Al_x\,Si_{(32-x)}O_{64}]$. There is, however, a significant charge unbalance in some cases (Table 5), which could possibly be due to an underestimation of fluorine in the presence of Al (or vice versa), although for the quantitative determination of fluoride sodium citrate and oxalate were added as complexing agents to avoid the formation of Al−F complexes.[10] Alternatively, it could also be due to the presence of a small concentration of either uncharged organic molecules or connectivity defects.

(14) Camblor, M. A.; Villaescusa, L. A.; Díaz-Cabañas, M. J. *Top. Catal.* **1999**, *9*, 59.

(15) Koller, H.; Wölker, A.; Villaescusa, L. A.; Díaz-Cabañas, M. J.; Valencia, S.; Camblor, M. A. *J. Am. Chem. Soc.* **1999**, *121*, 3368.

Table 4. Synthesis Results at 448 K for Reaction Mixtures with Varying Amounts of Benzylquinuclidinium Cations or Fluoride Anions[a]

H_2O/SiO_2	F^-/SiO_2	Al/(Si + Al) × 100	BQ/SiO_2	BQ/H_2O[b]	time (days)	pH	yield (g of solid/100 g)	product
3.6	0.5	0	0.5	0.122	6	8.9	27.3	Beta
7.5	0.5	0	0.5	0.063	6	8.5	16.3	ITQ-4
7.5	0.5	0	1	0.125	5	8.6	10.0	Beta + ITQ-4 (<10%)
					12	8.5	9.8	Beta + ITQ-4 (<10%)
7.5	0.5	2.56	0.53	0.066	6	8.5	20.3	Beta
7.5	1.0	0	0.5	0.063	6	7.4	12.7	ITQ-4
7.5	0.35	0	0.5	0.063	6	9.2	17.4	ITQ-4
7.5	0.075	0	0.5	0.063	6	8.3	18.1	amorphous
					20	8.3	20.6	ITQ-4 (<50%)
					34	8.2	18.1	ITQ-4 (<50%)

[a] The overall chemical composition changes here with respect to that reported in the Experimental Section. An increase in the BQ/SiO_2 ratio is achieved by additional BQ in its chloride form; an increase in the F/SiO_2 ratio is obtained by additional NH_4F. When the F/SiO_2 ratio is decreased below 0.5, HCl is added to maintain an $(HF + HCl)/SiO_2$ ratio of 0.5. [b] Unlike the H_2O/SiO_2 ratio case (see Experimental Section), for the calculation of the BQ/H_2O ratio all the water (including that coming from the neutralization of BQ(OH) with the acid) was considered.

Table 5. Chemical Composition of ITQ-4 Samples

Al/(Si + Al) in reaction mixture	Al/uc	N/uc	F/uc	C/N
0.00	0	1.98	2.11	14.1
0.0105	0.44	2.11	1.15	14.0
0.0205	0.68	2.12	0.61	13.9
0.0305	0.92	2.18	0.75	13.8
0.0370	1.23	2.14	0.49	13.9
0.0795	1.52	2.21	0.35	12.8

Calcination in air removes the organic and fluorine,[16] opening the microporous void space of the zeolites, which remain highly crystalline. The N_2 adsorption isotherms at 77 K (not shown) present the characteristic shape corresponding to adsorption on microporous solids. The microporous void volumes (0.20 ± 0.01 cm^3/g, as derived by the t-plot method) showed no significant deviations for any Al content in the zeolite between 0 and 1.52 Al per unit cell. Thus, the channels of calcined ITQ-4 are not blocked with extraframework Al species, at least with respect to N_2 adsorption.

Figure 3 illustrates the characteristic elongated prismatic shape of the crystallites, their relatively narrow distribution, and the increase in the aspect ratio with the Al content along with the decreasing crystal size as the Al content increases.

The morphology and crystal size of zeolite catalysts are of importance in reactions limited by diffusion of the reacting molecules within the intrazeolite void space. There is a very small increase in the aspect ratio for Al contents up to around 1/uc, while the crystallites become considerably more elongated as the Al content increases beyond that level of substitution (Figure 4). Because the aspect ratio is a consequence of the relative rate of growth of different faces, it can be argued that the incorporation of fluoride tends to decrease, or the incorporation of aluminum tends to increase, the relative rate of growth along the longest direction of the crystallites (which, from the preferred orientation correction applied during the Rietveld refinement of the pure silica phase,[8] corresponds to the direction of the channels). According to Gies,[17] the needlelike morphology generally observed in zeolites with monodimensional channels is a consequence of a slow rate of adsorption of the guest organic molecule, which controls the formation of new channels, while the buildup of the framework along the direction of an existing channel is faster. In the case of ITQ-4, the smaller aspect ratio observed for low Al contents (and hence higher F contents) in the zeolite may be a consequence of the tendency of F to be incorporated in the $[4^35^26]$ cages incorporating negative charges all around the channels, which may favor the deposition of organic cations and the formation of new channels adjacent to those previously formed.

It is noticeable that the data reported in Figure 4 is for both seeded and unseeded syntheses, suggesting seeding has no influence on the crystallite morphology and aspect ratio but merely reduces the crystallization time. Furthermore, we have observed that the crystal size of ITQ-4 materials synthesized in the presence of large seed crystals of pure silica ITQ-4 ($2 \times 2 \times 4$ μm^3) is always smaller than the seeds, indicating that the crystallization does not occur by mere growth of the seed crystals.

The isomorphous substitution of Si by Al in ITQ-4 can be confirmed by a number of techniques. The unit cell volumes of the calcined samples increase as the Al content increases (Figure 5, Table 6), which can in principle be due to the fact that the Al−O bond distance is larger than the Si−O distance. This correlation for the calcined materials appears to be approximately linear and the effect of Al incorporation is nearly isotropic as all the a, b, and c edges of the unit cell show similar variations (Table 6). The as-made samples also show an increase in volume with the increase in Al content (Figure 5), although this trend is not linear: while there is a linear variation for Si/Al ratios up to about 30, further increase in Al content produces a much larger increase of the unit cell volume. Additionally, the effect of Al incorporation is markedly anisotropic (see Table 6). This is possibly due to the effect of fluoride on the TOT angles caused by both its entrapment inside small cages and also its direct interaction with framework Si.

^{27}Al MAS NMR spectroscopy shows the presence of tetrahedral Al (characteristic chemical shift in the range 55−60 ppm) in both the as-made and calcined and rehydrated aluminosilicate samples (Figure 6), suggesting that isomorphous substitution of Si by tetrahedral Al occurred in ITQ-4. In the calcined samples there is another broad signal of low intensity near 0 ppm, which

(16) Villaescusa, L. A.; Barrett, P. A.; Camblor, M. A. *Chem. Mater.* **1998**, *10*, 3966.

(17) Gies, H. In *Inclusion Compounds*; Atwood, J. L., Davis, J. E. D., McNicol, D. D., Eds.; Oxford University Press: Oxford, 1991; Vol. 5, p 1.

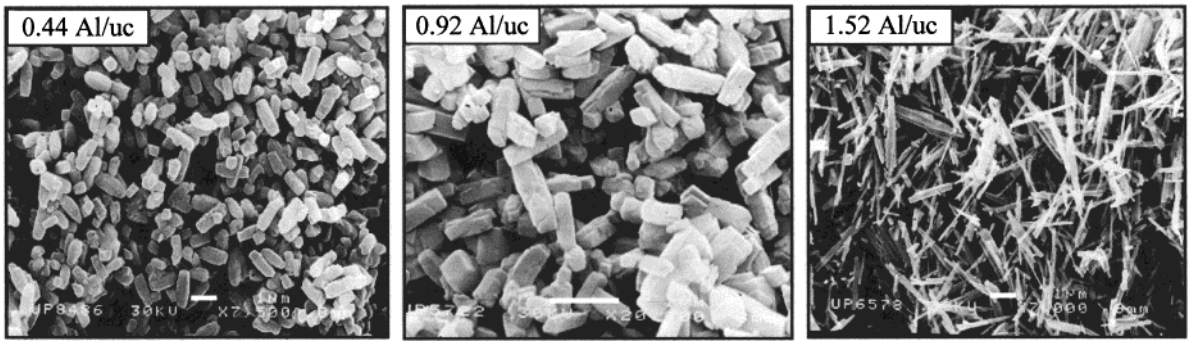

Figure 3. SEM pictures of ITQ-4 zeolites with the Al contents shown in each picture. The three zeolites were prepared using ITQ-4 seeds and have average particle sizes of around 1 × 0.5 × 0.5, 0.8 × 0.4 × 0.4, and 1.8 × 0.1 × 0.1 μm^3, respectively, from left to right. Scale bars represent 1 μm.

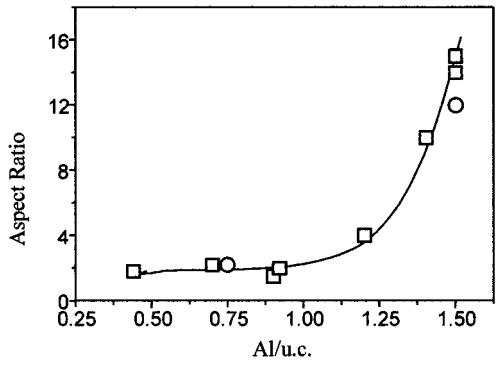

Figure 4. Aspect ratio of the ITQ-4 crystallites as a function of the Al content of the zeolites prepared with (squares) or without (circles) ITQ-4 seeds.

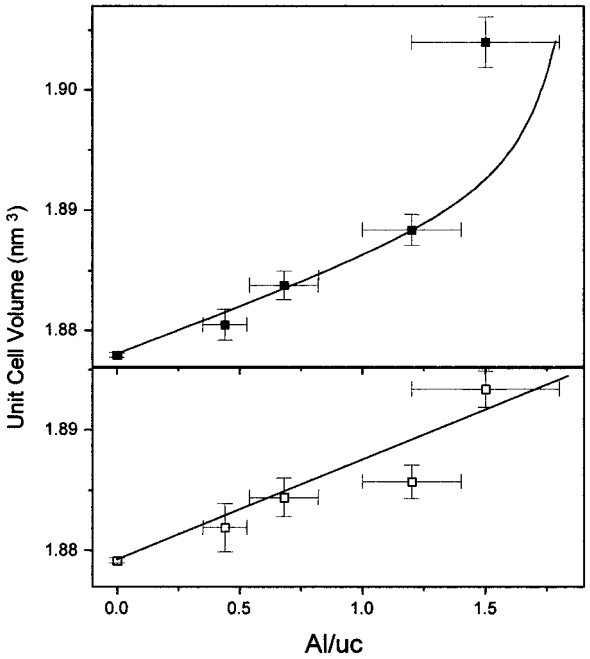

Figure 5. Dependence of the unit cell volume on the Al content of as-made (filled symbols) and calcined (open symbols) ITQ-4 zeolites. The (experimental) volume for 0 Al/uc differs from the one in ref 3, which was obtained by DLS minimization of the framework.

is assigned to octahedral Al in a very asymmetric environment, possibly produced by partial dealumination of the samples during the calcination. Quantification of the degree of dealumination by ^{27}Al MAS NMR was not carried out because of the known difficulties for quadrupole nuclei such as ^{27}Al.

Figure 7 shows the ^{29}Si MAS NMR spectra of calcined ITQ-4 samples. A loss of resolution is observed when the Al content of the material increases, although it is noticeable that even for the zeolite with the highest Al content several lines in the Si(OSi)$_4$ region, assigned to different crystallographic sites,[1] are evident. The loss of resolution can be attributed to a nonordered incorporation of Al in the framework with a concomitant decrease of local order, although a contribution from dealumination processes can also be expected. Another minor contribution to the loss of resolution can be heteronuclear coupling of ^{29}Si with ^{1}H. The spectra of the aluminosilicate samples also present some broad resonances in the −98 to −106 ppm region and a deconvolution showed the presence of at least two broad lines in this region: ca. −100 ppm (assigned to Si(OSi)$_3$OH defective groups) and ca. −103 ppm (assigned to Si(OSi)$_3$OAl groups). Although the severe overlapping of peaks hampers a reliable quantitative determination of the framework Si/Al ratio and of the concentration of defect groups, the spectra in Figure 7 suggest both the isomorphous substitution of Si by Al and the occurrence of dealumination processes during the calcination step. The ^{29}Si MAS NMR spectra in Figure 7 differ considerably from the one reported for MCM-58.[7] Not only is the resolution better for Al-ITQ-4 (for comparable Al content), but also the intensity distribution in the Q^4 region is not the same, which may hint at a difference in Al distribution.

Because of the absence of alkali cations in the material, the isomorphous substitution of Si by Al in the ITQ-4 framework gives rise after calcination to Brønsted acidity, without any need for ion exchange procedures. The acidity can be monitored by FTIR of the outgassed calcined materials in the hydroxyl stretching region followed by pyridine adsorption and desorption at increasing temperatures. As shown in Figure 8, the calcined dehydrated materials show four absorption bands in the hydroxyl stretching region at around 3742, 3694, 3629, and 3488 cm^{-1}. The band near 3742 cm^{-1} is typical of OH groups in silanols not involved in hydrogen bonding, for example, SiOH groups on the outer external surface. The band at 3629 cm^{-1} is characteristic of zeolitic Brønsted acid sites in framework hydroxyl Si−(OH)$^+$−Al bridges, and its acidity is confirmed by pyridine adsorption (Figure 9). The small band near 3694 and the broad one at 3488 cm^{-1} are more difficult to assign. The first one, which is nonacidic as shown by FTIR after adsorption of pyridine and

Table 6. Unit Cell Parameters of As-Made and Calcined ITQ-4 in the Topological Symmetry *I*2/*m*[a] with Estimated Standard Deviations in Parentheses

Al/uc	*a* (Å)	*b* (Å)	*c* (Å)	*β* (deg)	*V* (Å^3)
		As-Made			
0[b]	18.49612(10)	13.44060(5)	7.71112(5)	101.5768(5)	1877.98(19)
0.44(9)	18.577(7)	13.4274(4)	7.694(3)	101.520(15)	1880.5(1.3)
0.68(14)	18.611(6)	13.4301(4)	7.6920(22)	101.53(3)	1883.8(1.2)
1.2(2)	18.628(6)	13.4444(4)	7.6966(24)	101.572(14)	1888.4(1.3)
1.5(3)	18.699(9)	13.4815(8)	7.708(4)	101.51(5)	1904.0(2.1)
		Calcined			
0[b]	18.65243(13)	13.49597(8)	7.63109(6)	101.9781(5)	1879.17(20)
0.44(9)	18.667(9)	13.5028(6)	7.633(4)	102.005(12)	1881.9(2.0)
0.68(14)	18.677(7)	13.5100(5)	7.635(3)	102.006(19)	1884.4(1.6)
1.2(2)	18.686(7)	13.5234(5)	7.631(3)	102.067(18)	1885.7(1.4)
1.5(3)	18.705(7)	13.5448(5)	7.743(3)	102.095(18)	1893.4(1.5)

[a] The symmetry of as-made pure silica ITQ-4 has been recently found to be *Im* by microdiffraction using synchrotron radiation.[31] [b] From Rietveld refinement of synchrotron data.

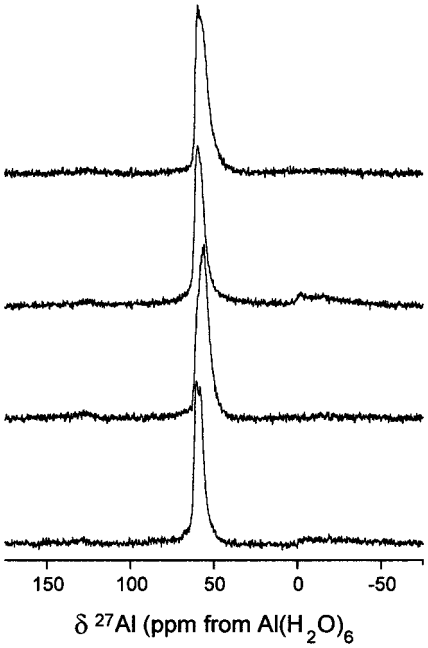

Figure 6. ^{27}Al MAS NMR spectra of ITQ-4 zeolites: (from bottom to top) calcined and as-made with 0.50 Al/uc and calcined and as-made with 1.52 Al/uc.

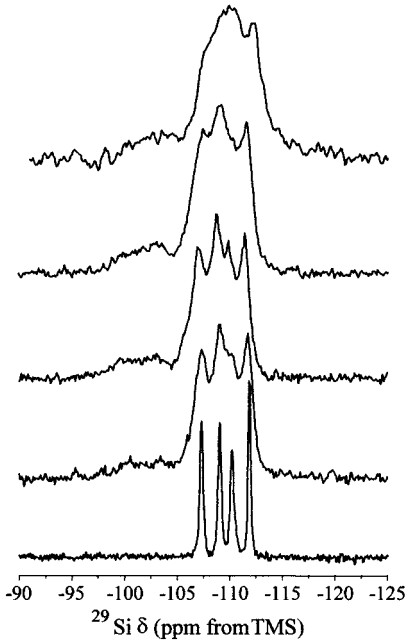

Figure 7. ^{29}Si MAS NMR spectra of calcined ITQ-4 samples with Al/uc contents of 0, 0.75, 0.92, 1.40, and 1.52 (from bottom to top).

desorption at 523 K (Figure 9), could be attributed to hydroxyl groups in Al species extracted from the framework during the calcination. However, its intensity shows no correlation with the Al content (the band is already present in the sample with no Al), and we could instead assign it to surface Si−OH groups in which the oxygen is involved in a weak hydrogen bond to an adjacent Si−OH, as found also in Al-free Ti-Beta synthesized in the fluoride medium.[18]

The broad band at around 3488 cm^{-1} deserves special attention. It appears within the typical region where strong hydrogen bonds are expected. However, this band appears to correspond to acidic hydroxyls, as shown by pyridine adsorption and desorption at 523 K (Figure 9): this band disappears and a very broad band in the region 3400−3700 cm^{-1} (corresponding to silanols involved in strong hydrogen bonds) is revealed. At first sight, assigning the 3488-cm^{-1} band to bridging Si−(OH)$^+$−Al species seems unrealistic because its position

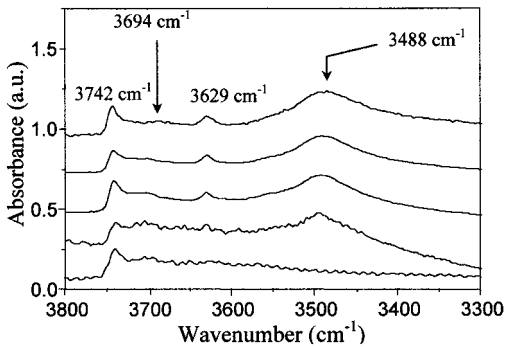

Figure 8. Infrared spectra in the OH stretching region of calcined ITQ-4 samples after outgassing (see Experimental Section). The Al content per unit cell is, from bottom to top, 0, 0.44, 0.68, 0.92, and 1.64.

is clearly at odds with the known range of vibration for bridging hydroxyls in zeolites (typical stretching region 3660−3600 cm^{-1}). A sensible interpretation of this band could be that it is due to hydrogen-bonded Si−(OH)$^+$−Al and Si−OH groups, so after pyridine adsorption on the bridging hydroxyl groups only the band due to hydrogen-bonded silanols appears, and it is shifted

(18) Blasco, T.; Camblor, M. A.; Corma, A.; Esteve, P.; Guil, J. M.; Martínez, A.; Perdigón-Melón, J. A.; Valencia, S. *J. Phys. Chem. B* **1998**, *102*, 75.

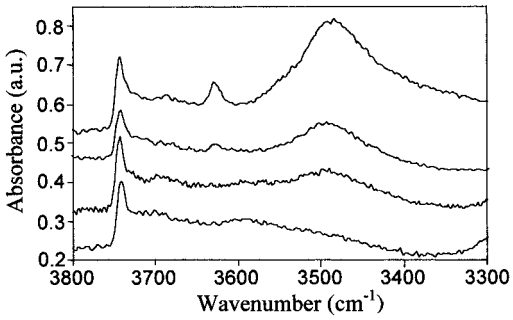

Figure 9. Infrared spectra in the OH stretching region of calcined ITQ-4 (1.64 Al/uc). The upper trace was recorded after outgassing at 673 K under vacuum. The rest of the spectra correspond to the same sample after pyridine adsorption and desorption at increasing temperatures (from bottom: 523, 623, and 673 K).

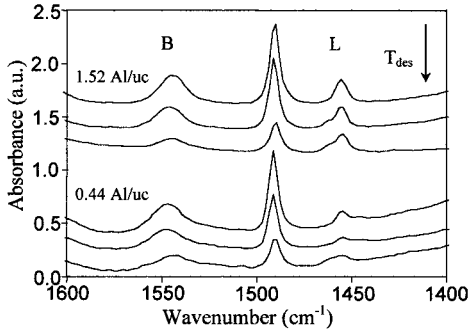

Figure 10. Infrared spectra in the vibrational region for pyridine molecules adsorbed on Brønsted (B) or Lewis (L) sites of two Al-ITQ-4 samples. For each sample, the traces correspond to desorption temperatures of (from top to bottom) 523, 623, and 673 K.

toward its typical position (broad band in the 3500−3600-cm^{-1} region). A similar broad band at 3495 cm^{-1}, which also disappears upon adsorption of pyridine, has been found in Al−STF[19] and Al−SSZ-24.[20] One important result of the FTIR experiments after adsorption of pyridine (Figure 9) is that, even for the sample with the highest Al content, essentially all the acidic hydroxyls are accessible to pyridine, supporting the conclusion that calcination does not cause any noticeable pore blockage, despite the monodimensional nature of the channels in ITQ-4.

After pyridine adsorption, the bands due to the pyridinium ion (i.e., pyridine adsorbed on Brønsted sites) and to pyridine coordinated to Lewis sites appear in the 1450−1650-cm^{-1} region[21] (Figure 10). The area of the bands at 1455 and 1545 cm^{-1} can be used to quantify the relative amount of Brønsted and Lewis sites, respectively, in different samples as a function of the desorption temperature to obtain insight into the relative strength and number of each type of acid centers. The results shown in Table 7 evidence the presence of both Brønsted and Lewis sites in all the aluminosilicate ITQ-4 samples, with the amount of total acid sites increasing with the Al content. However, we must note here that we have some concerns about this method of characterization of acidity in zeolites. We

(19) Villaescusa, L. A.; Camblor, M. A., unreported results.
(20) Martínez-Triguero, J.; Díaz-Cabañas, M. J.; Camblor, M. A.; Fornés, V.; Maesen, Th. L. M.; Croma, A. *J. Catal.* **1999**, *182*, 463.
(21) Jacobs, P. A. *Carboniogenic Activity of Zeolites*; Elsevier: Amsterdam, 1977.

Table 7. Relative Amounts of Pyridine Still Retained on Brønsted and Lewis Acid Sites of Al-ITQ-4 after Desorption at Different Temperatures[a]

	523 K		673 K	
Al/uc	Brønsted	Lewis	Brønsted	Lewis
0.44	3.57	0.50	1.18	0.30
0.66	5.06	0.66	2.44	1.01
0.92	7.35	0.45	3.27	0.55
1.64	9.55	1.78	3.29	1.83

[a] Relative amounts of pyridine on Brønsted and Lewis sites determined by measuring the area of the IR peaks at 1550 and 1450 cm^{-1}, respectively, normalized with respect to the sample weight and given in arbitrary units (so they can only be compared within each particular acidity type).

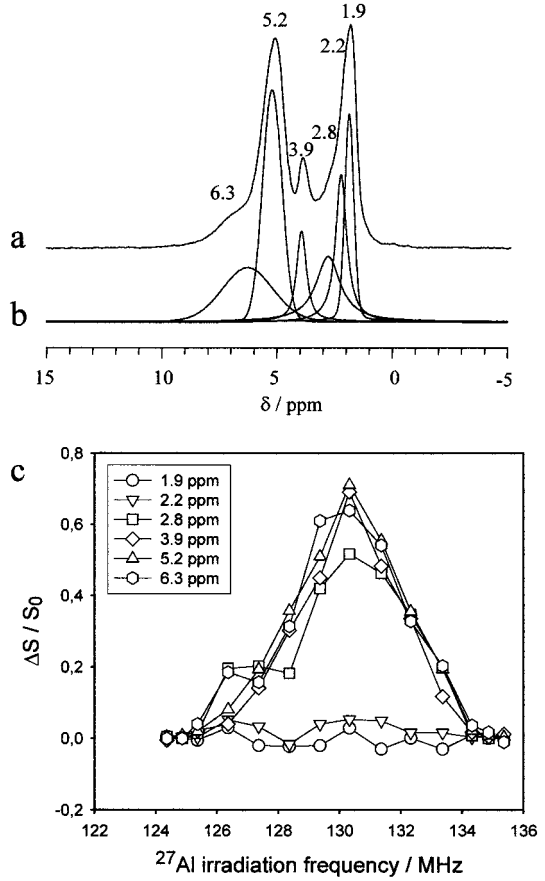

Figure 11. (a) ^{1}H MAS NMR spectrum of H-ITQ-4, (b) simulation components of experimental spectrum, and (c) $\Delta S/S_0$ values of all components in ^{1}H-^{27}Al REAPDOR experiment depending on ^{27}Al irradiation frequency.

frequently observe an increase in the amount of pyridine adsorbed on Lewis sites as the desorption temperature increases. Apparently, heating the zeolite in a vacuum in the presence of a base transforms some of the Brønsted sites into Lewis sites and this transformation does not revert back by cooling to room temperature (at which the spectra were recorded).

The interpretation of the IR band at 3488 cm^{-1} as arising from bridging Si−(OH)−Al groups is quite unusual, but it is substantially confirmed by solid-state NMR experiments that are presented in the following discussion. Figure 11a shows the ^{1}H MAS NMR spectrum of H-ITQ-4, revealing it to be composed of the six components shown in Figure 11b. According to a correlation between IR frequency and ^{1}H NMR chemical

shift,[22] these proton NMR lines can be clearly assigned to the IR bands discussed before. Using eq 4 in ref 22, the ^{1}H NMR lines at 1.9 and 2.2 ppm correspond to expected IR bands at 3755 and 3735 cm^{-1}, respectively, which are obviously the observed band at 3742 cm^{-1}. In a similar way, the ^{1}H NMR lines at 2.8 and 3.9 ppm are assigned to the bands at 3694 and 3629 cm^{-1}, respectively. From the two lines at 5.2 and 6.3 ppm two bands at 3531 and 3455 cm^{-1} are expected. These are obviously not resolved in the experiment because hydrogen bonds usually show rather broad IR signals. Hence, only one broad IR band at 3488 cm^{-1} is observed. Hydrogen-bonded acid sites were first reported by Beck et al. for ZSM-5.[23]

The static ^{27}Al spin−echo NMR spectrum of H-ITQ-4 (not shown) yields two lines, a broad quadrupolar component with a quadrupole coupling constant of 16 MHz and a narrower component. The broad component is due to bridging hydroxyl groups, as was first observed by Ernst et al.[24] on zeolite HY and H-ZSM-5, and confirmed by Hunger et al.[25] This large quadrupole coupling constant is explained by a bond distortion around the aluminum, especially the bond between Al, and the protonated oxygen atom is weakened by about a factor of 2.[26] The origin of the narrow ^{27}Al NMR component, which has also been observed by others (refs 24 and 25), can be explained by the presence of extraframework Al species (Lewis acid sites discussed before).

The local structure of the observed protons was further characterized using ^{1}H-^{27}Al double-resonance experiments. Double-resonance methods such as REDOR,[27] TRAPDOR,[28] or REAPDOR[29] are used to measure the heteronuclear dipole coupling, which is a direct function of the interatomic distance. The dipole coupling is normally averaged out by magic angle spinning, but it can be reintroduced into the evolution period of the aforementioned methods by disturbing the time evolution of the dipolar Hamiltonian in the periodic rotor spinning. The spectra acquisition is then performed under high-resolution conditions. The most prominent strategy in these methods is a set of two experiments. First, a rotor synchronized spin−echo NMR experiment is performed on the observed nucleus (here ^{1}H), and the intensity, S_0, is measured. In a second experiment, the spin−echo experiment is repeated with additional pulses on the coupled nucleus (here ^{27}Al). Because of these additional pulses, the dipolar Hamiltonian of the spatially close nuclei is not averaged out by MAS. This causes some loss of phase coherence in the spin−echo experiment, leading to a signal intensity, S, which is smaller than S_0 in the case of an effective dipole interaction between the two nuclei. The normalized intensity difference, $(S_0 - S)/S_0$, is a function of the dipolar evolution time (spin−echo time) and of the heteronuclear dipole interaction. In the case of isolated two spin pairs the interatomic distance can be determined by this method. Quadrupole nuclei, such as ^{27}Al, have several difficulties that can prohibit a quantitative analysis, but qualitative distance information can usually be unambiguously obtained.

Grey and Vega[28] have used the ^{1}H-^{27}Al TRAPDOR technique to show that the acidic protons in zeolite HY are spatially close to the aluminium which is characterized by a broad quadrupolar ^{27}Al NMR component. These authors investigated the proton-observed spectra by changing the ^{27}Al resonance offset of the dephasing pulses. By this mapping technique, information about the broadening of the ^{27}Al NMR resonance was indirectly obtained. Here, this mapping technique was carried out with the REAPDOR method, and the results are shown in Figure 11c. As expected, the ^{1}H NMR lines at 1.9 and 2.2 ppm do not show any coupling to ^{27}Al because they are assigned to nonacidic SiOH groups. All the other proton NMR lines show a dipole coupling to ^{27}Al, and the analysis of the offset behavior within a range of several MHz (Figure 11c) indicates that the corresponding ^{27}Al quadrupole coupling constant is ca. 16 MHz. Thus, the protons with ^{1}H chemical shifts of 2.8, 3.9, 5.2, and 6.3 ppm show a dipole coupling with the ^{27}Al component of the acid sites. The line at 2.8 ppm is assigned to extraframework AlOH or to hydrogen-bonded SiOH groups in the crystals. The ^{1}H-^{27}Al dipole coupling of these protons may arise from proximity to extraframework Al but also from acid sites in the neighborhood. The other three protons (3.9, 5.2, and 6.3 ppm) show a similar dipole coupling to ^{27}Al in acid sites, which proves that they are all of the same nature (bridging hydroxyl groups). These protons only differ in the strength of the hydrogen bond, which determines the ^{1}H chemical shift. This interpretation is in full agreement with the results from IR spectroscopy combined with pyridine adsorption.

Finally, the acidic properties of calcined Al-ITQ-4 were also investigated by temperature-programmed desorption of ammonia (TPD). The desorption curves for different Al contents show two desorption peaks separated by a constant temperature difference of around 418 K and assigned to ammonia physically and chemically adsorbed on ITQ-4 (low- and high-temperature desorption peaks, respectively). The amount and desorption temperature of each kind of adsorbed ammonia has been plotted versus the Al content in Figure 12. The amount of both types of adsorbed ammonia increases linearly with the Al content. The desorption temperatures also increase with the Al content. This change may be a consequence of the dynamic nature of the experiment and the increased difficulty in desorbing increasing amounts of ammonia. If the temperature of desorption is plotted against the NH_3 content (not shown) and the temperature for a zero loading is extrapolated, then we can get an idea of the desorption temperature in the absence of such diffusion problems. This extrapolated temperature of 573 K is smaller than the temperature obtained in the same way for the strongly acidic Al-ITQ-3 zeolite (593 K),[30] suggesting the acidity of ITQ-4

(22) Brunner, E.; Karge, H. G.; Pfeifer, H. *Z. Phys. Chem.* **1992**, *176*, 173.
(23) Beck, L. W.; White, J. L.; Haw, J. F. *J. Am. Chem. Soc.* **1994**, *116*, 9657.
(24) Ernst, H.; Freude, D.; Wolf, I. *Chem. Phys. Lett.* **1993**, *212*, 588.
(25) Hunger, M.; Horvath, T. *J. Am. Chem. Soc.* **1996**, *118*, 12302.
(26) Koller, H.; Meijer, E. L.; van Santen, R. A. *Solid State NMR* **1997**, *9*, 165.
(27) Gullion, T.; Schaefer, J. *J. Magn. Reson.* **1989**, *81*, 196.
(28) Grey, C. P.; Vega, A. J. *J. Am. Chem. Soc.* **1995**, *117*, 8232.
(29) Chopin, L.; Vega, S.; Gullion, T. *J. Am. Chem. Soc.* **1998**, *120*, 4406.
(30) Villaescusa, L. A. Ph.D. Thesis, Universidad Politécnica de Valencia, Spain, 1999.

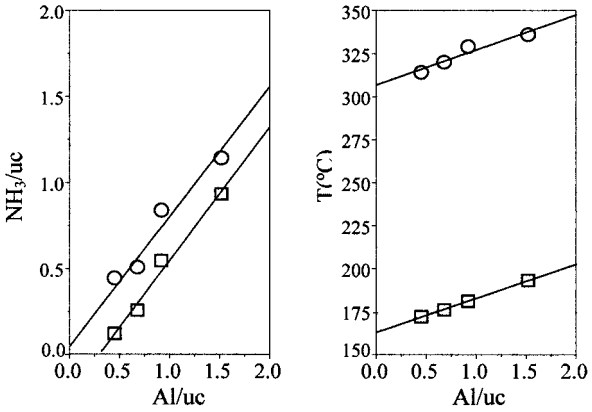

Figure 12. Amount of desorbed ammonia (left) and temperature of desorption (right, measured at the peak maxima) for Al-ITQ-4 as a function of the Al content. Circles and squares correspond to chemically and physically adsorbed ammonia, respectively.

is of medium strength. Comparison between the average desorption temperature of chemisorbed ammonia on ITQ-4 (598 K) and other zeolites[20] such as mordenite, ZSM-5, Y (Si/Al = 15−50), CIT-5, SSZ-24, and UTD-1 (745, 683, 623, 595, and 610 K, respectively) confirms this conclusion.

Conclusions

The phase selectivity during the crystallization of zeolites in fluoride media using benzylquinuclidinium as a structure-directing agent shows a strong dependency on both the Al and the water content of the reaction mixture. Two zeolites (Beta and ITQ-4) presenting large pore channels and a large void volume may be obtained as pure phases. The effect of increasing the Al content in the synthesis mixture on the phase selectivity is similar to the effect of decreasing its water content (both favoring the crystallization of zeolite Beta). By properly adjusting the water content, it is possible to synthesize these zeolites in a wide range of Si/Al ratios (10−∞ for Beta, 20−∞ for ITQ-4). The Al content in the reaction mixture determines not only the Al content in the zeolite but also the crystal size and, in the case of ITQ-4, the aspect ratio.

The isomorphous substitution of Si by Al in the framework of ITQ-4 has been proven by a number of chemical and physicochemical techniques: decrease in the fluoride content as the Al content increases, increase in unit cell volume, ^{27}Al and ^{29}Si MAS NMR spectroscopy, and acidity generated upon calcination. Al enters the framework in the form of $[AlO_{4/2}]^-$ tetrahedra at the expense of $[SiO_{4/2}F]^-$ units. Upon calcination, the organic and fluoride guests are removed and, while some dealumination takes place, no pore blockage occurs (as found not only by N_2 but also by pyridine adsorption). Calcined Al-ITQ-4 shows acidic properties of medium strength based on NH_3 desorption experiments. Three different acid sites could be resolved in the ^{1}H MAS NMR spectra with chemical shifts of 3.9, 5.2, and 6.3 ppm. The first line was correlated with the IR band at 3629 cm^{-1}, and the latter two lines correspond to a broad IR band at 3488 cm^{-1}. The close proximity between these protons and the distorted tetrahedral aluminum of the bridging hydroxyl Si−(OH)−Al groups was proven by ^{1}H-^{27}Al REAPDOR experiments.

Acknowledgment. The authors greatly acknowledge financial support by the Spanish CICYT (Project MAT97-0723) and by the Deutscher Akademischer Austauschdienst and the Spanish Ministry of Education and Science (Acciones Integradas, Project HA1999-0043). P.A.B. is grateful to the European Union TMR program for a postdoctoral fellowship.

CM001180E

(31) Bull, I.; Villaescusa, L. A.; Teat, S. J.; Camblor, M. A.; Wright, P. A.; Lightfoot, P.; Morris, R. E. *J. Am. Chem. Soc.* **2000**, *122*, 7128.